EXPERIMENTAL INVESTIGATIONS IN NONLINEAR VISCOUS BEHAVIOR OF SUBGRADE SOILS UNDER TRAFFIC-INDUCED LOADING

Jiang Li, Ph.D.
Assistant Professor
Department of Civil Engineering
School of Engineering
Morgan State University

National Transportation Center
Morgan State University
Baltimore, Maryland

August 1999

DISCLAIMER

The contents of this report reflect the views of the author, who is responsible for the facts and the accuracy of the information presented herein. This document is disseminated under the sponsorship of the Department of Transportation, University Transportation Centers Program, in the interest of information exchange. The U.S. Government assumes no liability for the contents or use thereof.

Technical Report Document Page

1. Report No.	2. Government Accession No.	3. Recipient's Catalog No.	
4. Title and Subtitle Experimental Investigations in Nonlinear Viscous Behavior of Subgrade Soils under Traffic-Induced Loading		5. Report Date August 1999 6. Performing Organization Code	
7. Author Dr. Jiang Li		8. Performing Organization Report No.	
9. Performing Organization Name and Address National Transportation Center Morgan State University 1700 E. Cold Spring Lane Baltimore, MD 21251		10. Work Unit No. (TRAIS) 11. Contract or Grant No.	
12. Sponsoring Organization Name and Address U.S. Department of Transportation Research and Special Programs Administration 400 7th Street, SW Washington, DC 20590-0001		13. Type of Report/Period Covered 14. Sponsoring Agency Code	

15. Supplementary Notes

Supported by a grant from the U.S. Department of Transportation, University Transportation Centers Program

16. Abstract

This paper concerns experimental investigations of nonlinear viscosity of subgrade soils under vehicle-induced loading. Subgrade soil samples—collected from the Soil/Aggregate Laboratory at the Geotechnical Exploration Division at the Maryland State Highway Administration, Maryland Department of Transportation—were used to conduct triaxial shear tests under repeated loading that is designed to simulate the cyclic stress induced by vehicles. Investigations in this paper included two aspects. First, a nonlinear viscous model has been introduced to describe the relation of shear stress and strain rate. This relation is reduced from the constitutive law of nonlinear poroviscosity suggested by Li (1994, 1999a, 1999b) and Li and Helm (1995, 1998). Second, to model the viscous behavior of soil under cyclic loading, constitutive parameters were investigated and calibrated through experimental results from triaxial shear tests. In this paper, viscous parameters were assumed to be a function of the deviatoric strain and loading repetitions. Viscous behavior of soils changing with deviatoric strain and cyclic loading repetition were studied.

17. Key Words	18. Distribution Statement		
Constitutive Relationship, Nonlinearity, Deviatoric and Spherical Stress, Deviatoric and Spherical Strain, Viscosity, Stress and Strain Invariance.			
19. Security Classification (of this report)	20. Security Classification (of this page)	21. No. of Pages	22. Price
Unclassified	Unclassified	47	

TABLE OF CONTENTS

ABSTRACT

This paper concerns experimental investigations of nonlinear viscosity of subgrade soils under vehicle-induced loading. Subgrade soil samples collected—from the Soil/Aggregate Laboratory at the Maryland State Highway Administration, Maryland Department of Transportation—were used to conduct triaxial shear tests under repeated loading that is designed to simulate the cyclic stress induced by vehicles. Investigations in this paper have included two aspects. First, a nonlinear viscous model is introduced to describe the relation of shear stress and strain rate. This relation is reduced from the constitutive law of nonlinear poroviscosity suggested by Li (1994, 1999a, 1999b) and Li and Helm (1995, 1998). Second, to model the viscous behavior of soil under cyclic loading, constitutive parameters were investigated and calibrated through experimental results from triaxial shear tests. In this paper, viscous parameters were assumed to be a function of the deviatoric strain and loading repetitions. Viscous behavior of soils changing with deviatoric strain and cyclic loading repetition were studied.

ACKNOWLEDGMENTS

This research program is sponsored by the National Transportation Center (NTC) at Morgan State University (MSU) through the 1999 Summer Research Grants. The principal investigator (P.I.) thanks Dr. Z. A. Farkas, the Interim Director of NTC, for his leadership and support in making the second phase of this research possible. The author thanks Dr. Ding, a senior visiting scholar, for his help in supervising students' laboratory activity; and Mr. Joseph Dwight, a senior student from the Department of Civil Engineering, for his involvement in this experimental investigation. The author also thanks the NTC staff (Mr. William Lowe, former Editor; Ms. Vivian Mason, present Editor; Ms. Anita Cook, Office Secretary; and Ms. Tawanda Nutt, Fiscal Administrator) for their kind support during this summer research program.

INTRODUCTION

The top priority for improving the nation's highway system is to focus on quality and performance of the roadway pavement. Both quality and performance of pavement will largely depend on the mechanical behavior of subgrade soils, especially the viscous response of subgrade soil under dynamic vehicle-induced loading. However, little effort has been made in investigating soil viscous behavior in both the laboratory and the field. In most numerical and computer modeling investigations, parameters related to soil viscous behavior are traditionally empirical. For example, computer modeling with the Finite Element Method is one of the most popular numerical methods currently used in computation of dynamic responses of pavement and subgrade under cyclic loading. In numerical modeling with the Finite Element Method, an extra viscous term, however, is simply added to the governing equation. It is assumed that material viscosity associates with the rigidity (or elastic modulus) of the material (Zienkiewicz, 1977). Similar approaches are used in other techniques of dynamic analysis. Therefore, former models are initially assumed as elastic ones and are then modified to the viscous-elastic models by adding an extra viscous term that empirically associates with material elasticity. A new constitutive law proposed in this research program does not need to apply the traditional *ad hoc* terms to modeling dynamic response of road subgrade (Li and Helm, 1997). The viscous stress-strain rate relation demonstrates elasto-viscous features when this new model is invoked and applied to the governing equation developed from the first principles of continuum mechanics. Verification of this constitutive law is conducted with laboratory investigations using the soil dynamic triaxial apparatus. Investigation of dynamic behavior of subgrade soil includes dynamic strength and failure, viscous stress-strain-time relation, creeping and fatigue due to repeated loading, and dynamic shear level at a low confining pressure. Such research is essential to enhance our understanding of the viscous behavior of subgrade soils under dynamic conditions due to traffic and nontraffic- induced loads.

In the present research, experimental investigations of nonlinear viscous behavior of subgrade soil under vehicle-induced loading are featured. The current research is the second phase of the research program funded by the National Transportation Center (NTC) at Morgan State University

through the 1998 Faculty Summer Research Grants. The first phase of this program emphasized laboratory studies in nonlinear elastic behavior of subgrade soils (Li, 1999a). The new nonlinear elastic modulus was assumed to be a function of repetition of loading and recoverable strain. Current research (i.e., the second phase of the research) will center on dynamic viscous responses of pavement subgrade. Viscous responses of subgrade soil under cyclic shearing play a central role in the performance of road surface, especially for dynamics such as cyclic stress induced by the vehicles. A new constitutive model is introduced in this investigation. This new relation of stress and strain rate assumes that the subgrade soil behaves as nonlinear poroviscous material (Li, 1994, 1999c) rather than the poroelastic material (Li, 1999a, 1999b). Thus, subgrade soil is assumed to behave as non-Newtonian flow. When the constitutive relation is combined with the first principles—such as conservation of momentum, mass, and energy—a governing equation is developed (Li and Helm, 1995). The complete mathematical description is a very powerful tool to describe elasto-viscous behavior of subgrade soil under both traffic and nontraffic-induced loads (Li and Helm, 1998). Investigation of the proposed research program includes dynamic strength and failure at a higher shear stress level and a lower confining pressure, shear viscosity, different time-dependent relations among stress σ, strain ε, and strain rate during loading and unloading, such as $\sigma - t - \varepsilon - \dot{\varepsilon}$, $\sigma - t - \varepsilon$, $\mu - t - \varepsilon$, $M_r - t - \varepsilon$. Constitutive parameters are to be investigated with the dynamic triaxial apparatus especially designed for testing subgrade and are calibrated from laboratory results of soil dynamic experiments. The possible correlation between nonlinear viscosity and elasticity has also been studied.

VISCOUS CONSTITUTIVE RELATIONSHIP

Relation of Viscous Stress and Strain Rate

If the relation of stress and strain rate for subgrade soil is assumed to be viscous, according to the theory of viscosity (Malvern, 1969), then the following expression results:

$$\boldsymbol{\sigma} = \mathbf{D}\dot{\boldsymbol{\varepsilon}}, \tag{1}$$

where $\boldsymbol{\sigma}$ and $\boldsymbol{\varepsilon}$ represent viscous stress and strain tensors that are the symmetric second-order tensors. The dot denotes the derivative with respective to time. The term **D** is a fourth-order tensor of viscosity for the constitutive law and can be defined as a function of stress, strain, rate of strain, time, space, and temperature for cases of physical nonlinearity. From the symmetry of the viscous stress and strain tensors and with an assumption of isotropic soil material, **D**, a fourth-order tensor in Equation 1, can be written as:

$$\mathbf{D} = (k - 2\mu/3)\boldsymbol{\delta}\boldsymbol{\delta} + \mu(\boldsymbol{\delta}\boldsymbol{\delta} + \boldsymbol{\delta}\boldsymbol{\delta}), \tag{2}$$

where $\boldsymbol{\delta}$ is the Kronecker delta, and κ and μ are the bulk and shear viscous parameters, respectively. It is known that, for subgrade soils, the stress-strain relation is normally *not* linear. This fact might suggest the relation between the viscous stress and strain rate might not be linear. Therefore, viscous parameters κ and μ in Equation 2 are not constant. Alternatively, Equation 1 can be written in the following two parts (Malvern, 1969):

$$\boldsymbol{\sigma} = tr\boldsymbol{\sigma}\boldsymbol{\delta}/3 + \boldsymbol{\sigma}^{\mathrm{D}} = \kappa tr\dot{\boldsymbol{\varepsilon}}\boldsymbol{\delta} + 2\mu\dot{\boldsymbol{\varepsilon}}^{\mathrm{D}}, \tag{3}$$

where the superscript D denotes a deviatoric variable, and *tr* denotes the trace of the stress tenor. The term $tr\boldsymbol{\sigma}/3$, where in Equation 3 it is the spherical or mean stress that is associated with volume strain rate $d\boldsymbol{\varepsilon}/dt$ in a form (k = 1, 2, and 3) (Malvern, 1969):

$$\mathrm{tr}\boldsymbol{\sigma}/3 = \kappa \mathrm{tr}\dot{\boldsymbol{\varepsilon}}. \tag{4a}$$

$\boldsymbol{\sigma}^{\mathrm{D}}$ is the second-order tensor of deviatoric or shear stress that is related to deviatoric strain rate tensor $d\boldsymbol{\varepsilon}^{\mathrm{D}}/dt$ by:

$$\boldsymbol{\sigma}^{\mathrm{D}} = 2\mu\dot{\varepsilon}^{D} \tag{4b}$$

For further investigations, Equations 4a and 4b are written in terms of invariants of stress and strain as follows (Malvern, 1969):

$$I_1 = 3\kappa\dot{J}_1, \tag{5a}$$

$$\sqrt{I_2^D} = 2\mu\sqrt{\dot{J}_2^D}, \tag{5b}$$

where I_1 (= $tr\boldsymbol{\sigma}$) and I_2^{D} (= $\boldsymbol{\sigma}^{\mathrm{D}}\boldsymbol{\sigma}^{\mathrm{D}}/2$) are invariants of the first spherical stress and the second deviatoric stress individually (Malvern, 1969). The terms dJ_1/dt (= $dtr\boldsymbol{\varepsilon}/dt$) and $\mathrm{d}J_2^{\mathrm{D}}/dt$ [= $(d\boldsymbol{\varepsilon}^{\mathrm{D}}/\mathrm{dt})(d\boldsymbol{\varepsilon}^{\mathrm{D}}/dt)/2$] represent the first spherical and the second deviatoric strain tensor invariants. The differential operator d/dt denotes the derivative with respect to time.

Stress and Strain in a Quasi–Three-dimensional Space

Normally, laboratory studies are conducted in a quasi-triaxial space. The quasi-triaxial space is a special case of true three-dimensional space. For the quasi-triaxial case and in the principal stress and strain spaces, there are principal stresses $\sigma_1 \neq \sigma_2 = \sigma_3$ and principal strains $\varepsilon_3 \neq \varepsilon_2 = \varepsilon_3$. Bearing in mind the definitions of $I_1 = tr\boldsymbol{\sigma}$ and $I_2^{\mathrm{D}} = \boldsymbol{\sigma}^{\mathrm{D}}\boldsymbol{\sigma}^{\mathrm{D}}/2$, then the stress-strain relations of Equations 5a and 5b are, respectively, reduced to:

$$(\sigma_1 + 2\sigma_3) = 3\kappa(\dot{\varepsilon}_1 + 2\dot{\varepsilon}_3), \tag{6a}$$

$$(\sigma_1 - \sigma_3) = 2\mu(\dot{\varepsilon}_1 - \dot{\varepsilon}_3). \tag{6b}$$

Equations 6a and 6b are relations of volume stress and shear stress versus volume and shear strain rate in a quasi-triaxial system. Since the bulk modulus κ is related the first stress

invariance, and confining stress of subgrade soils *in situ* is low, in this paper, Equation 6b is the main concern. Namely, the investigation of the relation between deviatoric stress σ_d(= $\sigma_1 - \sigma_3$) and deviatoric strain rate $\dot{\varepsilon}_d = \dot{\varepsilon}_1 - \dot{\varepsilon}_3$ is emphasized. The relation $\dot{\varepsilon}_d = \dot{\varepsilon}_1 - \dot{\varepsilon}_3$ needs to be simplified further for testing conditions in the laboratory. Either a negligible $\dot{\varepsilon}_3$ is assumed or a relation between $\dot{\varepsilon}_1$ *and* $\dot{\varepsilon}_3$ is assumed, for instance, associated by a constant (Li, 1999a). In most cases, the relation 6a can be evaluated by investigating the correlation between shear viscosity μ and volume viscosity κ. Such a relation of $\sigma_d = 2\mu(d\varepsilon_d/dt)$ can be conveniently applied to a quasi-triaxial apparatus. Since the viscosity is an important input parameter in highway pavement design and numerical modeling, the discussion of shear viscosity is emphasized in the later sections.

Nonlinear Viscous Parameters μ and κ

In this investigation, to consider viscous nonlinearity between viscous shear stress and shear strain rate, volume viscosity κ and shear viscosity μ are assumed to be functions of the stress and strain invariances (I and J) and the number of the repetition N, namely $\kappa = \kappa(I_1, N, J_1)$ and $\mu = \mu(I_1, N, J_2^D)$. The variable N is the number of repetitions for cyclic loading. If it is further assumed that the variables in the viscous parameters κ and μ can be independent from each other and are able to be expressed by the product of three independent functions, then $\kappa(I_1, N, J_1)$ and $\mu(I_1, N, J_2^D)$ are given by:

$$\kappa = \kappa_0(I_1)\kappa_1(N)\kappa_2(J_1), \tag{7a}$$

$$\mu = \mu_0(I_1)\mu_1(N)\mu_2(J_2^D). \tag{7b}$$

The three independent functions in Equations 7a and 7b indicate that the effects of these three variables on volume and shear viscosity κ and μ can be decoupled. The three functions do not affect each other, although volume and shear viscosity are functions of three variables. This assumption will be further discussed with experimental results that are shown later in the "Experimental Investigations in the Laboratory" section.

Keeping the assumption for Equations 7a and 7b in mind and further assume the nonlinear viscous parameters κ and μ to be power functions of *I*, *J*, and *N*, one has:

$$\kappa = a_0 (I_1)^{a_1} N^{a_2} (J_1)^{a_3} \tag{8a}$$

$$\mu = b_0 (I_1)^{b_1} N^{b_2} (J_2^D)^{b_3}, \tag{8b}$$

where a_i (i = 0, …, 3) and b_i (i = 0, … 3) are constants that can be calibrated from test results. *N* is the repetition of cyclic loading. Note that, in Equations 8a and 8b, I_1 is defined as initial mean confining pressure and is nondimensional and normalized by the unit atmosphere pressure (0.1 MPa). For convenience, the same notation is used later everywhere in this paper. If Equation 8 is compared with Equation 7, it is not difficult to find $\kappa_0 = a_{0I}(I_1)^{a_1}$, $\kappa_1 = a_{0N} N^{a_2}$, and $\kappa_1 = a_{0J}(J_1)^{a_3}$; and $\mu_0 = b_{0I}(I_1)^{b_1}$, $\mu_1 = b_{0N} N^{b_2}$, and $\mu_1 = b_{0J}(J_2^D)^{b_3}$, where $a_0 = a_{0I} a_{0N} a_{0J}$ and $b_0 = b_{0I} b_{0N} b_{0J}$. Again, in the quasi–three-dimensional space, the first stress invariance, the first strain invariance and the second deviatoric strain invariance become $I_1 = (\sigma_1 + 2\sigma_3)$, $J_1 = (\varepsilon_1 + 2\varepsilon_3)$, and $J_2^D = 2(\varepsilon_1 - \varepsilon_3)$. Accordingly, Equations 8a and 8b reduce to:

$$\kappa = a_0 (\sigma_1 + 2\sigma_3)^{a_1} N^{a_2} (\varepsilon_1 + 2\varepsilon_3)^{a_3} \tag{9a}$$

$$\mu = b_0 (\sigma_1 + 2\sigma_3)_1^{b_1} N^{b_2} (\varepsilon_1 - \varepsilon_3)^{b_3}. \tag{9b}$$

Although the same notation b_0 is used in Equations 9b and 8b, b_0 in Equation 9b equals 8^{b3} times b_0 in Equation 8b because of $J_2^D = 2(\varepsilon_1 - \varepsilon_3)$. If the term b_0 is not specified, then the notation b_0 in Equation 9b is to be adopted in later discussions through this report. In the present investigations, Equation 9b is emphasized and verified through laboratory experiments. Further investigations are to calibrate constitutive parameters (i.e., b_0, b_1, b_2, and b_3) from test results.

Governing Equation with the Constitutive Relation

If the first principles such as conservation of momentum, mass, and energy, are invoked, a governing equation can be developed. The governing equation for soil particle deformation with consideration of viscous drag force due to pore water flow is given as (Li, 1994; Li and Helm, 1995, 1998):

$$c_1\ddot{\mathbf{u}} + \dot{\mathbf{u}} + \mathbf{c}_2\nabla(\mathbf{DL}\dot{\mathbf{u}}) = \mathbf{R}, \tag{10}$$

where two dots indicate the second derivative with respect to time, **L** is a matrix for definition of strain, and **u** is the displacement field of the solid phase. The right-hand side vector **R** is defined by:

$$\mathbf{R} = c_3\mathbf{b} + c_4\dot{\mathbf{q}}^{\mathrm{b}} + \mathbf{q}^{\mathrm{b}} + c_5, \tag{11}$$

where coefficients c_i(i = 1, ..., 5) are coefficients of the governing Equation 6. The vectors **b** and $\mathbf{q}^{\mathrm{b}}$ denote the body force and the bulk flux [$\mathbf{q}^{\mathrm{b}} \equiv n\mathbf{v}^{\mathrm{w}} + (1 - n)\mathbf{v}^{\mathrm{s}}$]. The divergence of $\mathbf{q}^{\mathrm{b}}$ can be further reduced to zero by invoking the incompressibility conditions of solid grain and pore fluid (i.e., the second and third terms on the right-hand side of Equation 11 become zero due to $\nabla\mathbf{q}^{\mathrm{b}}$ = 0). The nonlinear viscous relation is introduced to the governing equation (the third terms on the left- hand side of Equation 10). Applying the definition given in Equation 8, one can find the alternative form:

$$c_1\ddot{\mathbf{u}} + \dot{\mathbf{u}} + \mathbf{c}_2[\dot{\mathbf{D}}\nabla(\mathbf{Lu}) + \mathbf{D}\nabla(\mathbf{L}\dot{\mathbf{u}})] = \mathbf{R}, \tag{12}$$

where the third and fourth terms equal

$$\nabla(\mathbf{DL}\dot{\mathbf{u}}) = [\dot{\mathbf{D}}\nabla(\mathbf{Lu}) + \mathbf{D}\nabla(\mathbf{L}\dot{\mathbf{u}})], \tag{13}$$

in which the first term is equivalent to the traditional elastic term, and the second term is similar to the viscous term in the elastic-viscous model. Equations 1, 2, and 8 were derived by Li (1994) and Li and Helm (1995, 1998). One may note that the coefficient of the third term on the right-hand side of Equation 12 plays an equivalent role as Young's modulus in the elastic model and theory. From Equation 13, it is suggested that the viscous matrix **D** is associated with the "apparent Young's modulus" by taking the derivative of **D** with respect to time. The last term on the right-hand side of Equation 12 is the typical viscous term. Equation 12 is a powerful tool to analyze dynamic response of subgrade soil under traffic loading. With the technology of numerical analysis, such as the Finite Element Method or the Boundary Element Method, the governing Equation 12 can be applied to engineering and solve problems with specific boundary conditions. The third and the fourth terms in Equation 12 are, however, not *ad hoc* but are derived from the constitutive relation related to Equations 1, 2, and 8. This fact will set the governing Equation 13 with a nonlinear viscous model from the traditional viscous-elastic model. The further investigation will verify the relation in Equation 13 between deviatoric components.

EXPERIMENTAL INVESTIGATIONS IN THE LABORATORY

Samples Preparation and Basic Properties

Subgrade soil samples are received from the Soil/Aggregate Laboratory at the Geotechnical Exploration Division at the Maryland State Highway Administration, Maryland Department of Transportation. These subgrade soil samples were originally collected from two sites in Howard County, Maryland. The main physical properties of the samples from two sites are listed in Table 1a. Sample preparation for testing the resilient modulus follows the code of AASHTO T292-91.

Equipment and Test Conditions

Experimental investigations have been conducted at the Geotechnical Laboratory at the Department of Civil Engineering, School of Engineering, Morgan State University. Samples were tested with the triaxial apparatus (RMT HX1000) that is specially designed for testing the subgrade soil under cyclic loading by the Structure Behavior Laboratory Equipment, Inc. Samples were first subjected to a conditioning period with zero confining pressure. Then, the samples were subjected to dynamic loading with the undrained condition (UU conditions). The magnitude of the repeated loading increases with a constant number of repetitions in each sequence. More information on the testing conditions is listed in Table 1b.

Test Results and Parameter Calibration

After samples have been tested, acquired test data are retrieved from the computer, analyzed, and plotted in several sets of family curves, among which the following relations are characterized.

Relation of stress over strain rate versus strain ($\sigma / \dot{\varepsilon}_d - \varepsilon_d$)

The nonlinear relation of deviatoric stress over strain versus deviatoric strain ($\sigma / \dot{\varepsilon}_d - \varepsilon_d$) is given in Figures 1a and 1c for two groups of samples. In Figures 1a and 1c, each curve of the stress over strain rate (i.e., viscosity) decreases with an increase of the deviatoric strain. Simultaneously, each curve decreases with an increase of repetition *N*. Applying the technology

of curve fitting to the data curves in Figures 1a and 1c, finds that the trend curves (the dashed lines in the figures) follow a pattern of the power function [i.e., $f(x) = ax^b$]. The calibrated parameters (i.e., b_0, b_2, and b_3) are listed in Tables 2a and 2b. Details of calibration to obtain the constitutive parameters will be discussed in the "Discussion and Analysis of Results" section. Since the confining pressure used in the investigation equals the unit atmosphere, the normalized first stress invariance $I_1 = 1.0$ (i.e., in this paper, the first stress invariance is normalized by the unit atmosphere that equals 0.1 MPa), and b_0 equals the product of b_{0N} and b_{0J}. The relation of the parameter versus N is illustrated in Figures 1b and 1d.

Relation of stress over strain versus strain ($\sigma_d / \varepsilon_d - \varepsilon_d$)

The nonlinear relation of deviatoric stress versus recoverable strain rate is illustrated in Figures 2a and 2c, in which each curve of stress versus strain rate also changes with the repetition N of periodic loading. If compared with the relation of stress over strain rate versus strain shown in Figures 1a and 1c, the curve of stress over strain versus strain ($\sigma_d / \varepsilon_d - \varepsilon_d$) has the same pattern as Figures 1a and 1c. Namely, stress over strain versus strain ($\sigma_d / \varepsilon_d - \varepsilon_d$) decreases nonlinearly with an increase of deviatoric strain. At the same time, for a value of strain, deviatoric stress over strain decreases with an increase of repetition N. Similarly, the method of curve fitting for the power function is used to find the parameters. A set of calibrated parameters (i.e., k_0, k_2, and k_3) is listed in Tables 3a and 3b. The stress over strain versus strain ($\sigma_d / \varepsilon_d - \varepsilon_d$) is equivalent to the resilient modulus versus strain ($M_r - \varepsilon_d$) if elastic theory is applied as Li (1999a) suggests.

Relation of Stress Versus Strain ($\sigma_d - \varepsilon_d$)

The nonlinear relation of deviatoric stress versus recoverable strain depicted in Figures 3a and 3c, in which each stress-strain curve changes with the number of periodic loading N and deviatoric strain. From Figures 3a and 3c, deviatoric stress increases nonlinearly with an increase of deviatoric strain, whereas for a given value of deviatoric strain, deviatoric stress declines with an increase of the loading repetition N. Although the curves ($\sigma_d - \varepsilon_d$) are different

from the two groups $\sigma_d / \dot{\varepsilon}_d - \varepsilon_d$ and $\sigma_d / \varepsilon_d - \varepsilon_d$ previously discussed, the trend curves still follow the pattern of the power function. With the curve-fitting method, parameters (i.e., n_0, n_2, and n_3) are calibrated and listed in Tables 4a and 4b.

DISCUSSION AND ANALYSIS OF RESULTS

From the previous section, test data from experimental investigation are demonstrated in Figures 1 through 3, and the parameters are calibrated and listed in Tables 2 through 4. The following discussion is based on results from experimental investigations.

Stress Over Strain Rate as a Function of N and ε_d

Recalling the relation given by Equation 4b, viscous stress over strain rate versus N and ε_d (i.e., $\sigma_d / \dot{\varepsilon}_d - N - \varepsilon_d$) is the relation of viscosity μ changing as a function of N and ε_d [i.e., $\mu(N, \varepsilon_d)$ or $\mu - N - \varepsilon_d$]. Assuming the test condition $f(I_1) = b_{0I}(I_1)^{b_1} = 1.0$ and invoking Equation 6b, one finds that the shear viscous stress has the following nonlinear relation with the strain rate in the quasi-triaxial space:

$$\sigma_d / \dot{\varepsilon}_d = 2\mu(N, \varepsilon_d) = 2(b_0 N^{b_2} \varepsilon_d^{b_3}), \tag{14}$$

where μ in Equation 14 equals:

$$\mu(N, \varepsilon_d) = b_0 N^{b_2} \varepsilon_d^{b_3}, \tag{15}$$

in which the terms b_0, b_2, and b_3 are constitutive parameters; b_0 has a dimension of kPa-second; and b_2 and b_3 are dimensionless. For simplicity, b_0 is assumed to be a constant in this paper; although, in a more general case, b_0 can be a function of N and confining pressure. With Equation 7b, the functions of $\mu_1(N)$ and $\mu_2(J^D_2)$ have been introduced as the following two forms:

$$\mu_2(N_i) = b_{0N} N^{b_2}, \tag{16a}$$

$$\mu_3(\varepsilon_d) = b_{0J} \varepsilon_d^{b_3}, \tag{16b}$$

As described previously, parameters b_0, b_2, and b_3 can be calibrated from experimental results. The procedure of calibration for constitutive parameters involves two steps. The first step is to find b_3 and $b_0 N^{b_2}$ from each curve. The calibrated parameter b_3 is listed in Tables 2a and 2c in

which R^2 is given the regression of test data (for a perfect match of trend curve, R^2 = 1.0). The second step is to find b_2 and b_3 using the set of data $b_0 N_i^{\ b2}$ and N_i in Tables 2a and 2b. The calibrated parameters b_0 and b_2 are given in Table 2b for six samples from two groups. To analyze the test results without considering the effect of repetitions, the deviatoric stress σ_d can be divided by $f_1(N)$ [i.e., σ_d / N^{b_2}]. From this, the relation σ_d / N^{b_2} against ε_d is drawn (Li, 1999a). For a special case of a negligibly small b_2, there is no effect of the loading repetition N on the relation of stress versus strain rate. Moreover, for a special case of negligibly small coefficients b_2 and b_3 (i.e., both $b_2 \approx 0$ and $b_3 \approx 0$), the relation described in Equation 15 becomes constant; and Equation 14 reduces to the relation of linear viscosity. Thus, the nonlinear relation Equation 14 reduces to a linear one: $\sigma_d = b_0 \dot{\varepsilon}_d$. From Figures 1 and 2, one can observe how parameters b_2 and b_3 affect the curves $\sigma / \dot{\varepsilon}_d - N - \varepsilon_d$. The expressions based on the calibrated parameters are given below:

Group DJ0: $$\sigma_d / \dot{\varepsilon}_d = 16706 N^{-0.43} \varepsilon_d^{-0.23} \quad \text{(kPa)} \qquad (17a)$$

Group DJ50: $$\sigma_d / \dot{\varepsilon}_d = 2172 N^{-0.34} \varepsilon_d^{-0.55} \quad \text{(kPa).} \qquad (17b)$$

From Equations 17a and 17b, it is clear that viscosity of subgrade soils from the two groups decreases dramatically when subgrade soils undergo a long period shear force and large deformation.

Stress Over Strain as a Function of *N* and ε_d

An interesting topic to discuss is the relation of stress over strain as a function of N and ε_d (i.e., $\sigma_d / \varepsilon_d - N - \varepsilon_d$). Previous investigations, with emphasis on nonlinear elasticity, were conducted by Li (1999b). As described previously in the early discussion of this research report (see Equation 13), effort to investigate the correlation of viscosity and elasticity will be made in this section. Namely, the relation of stress over strain as a function N and ε_d in Figures 2a and 2c, as well as its correlation with viscosity μ versus strain in Figures 1a and 1c, are discussed. The relation of stress over strain versus strain inherently is the relation resilient modulus M_r versus strain (i.e., $M_r - N - \varepsilon_d$), if one applies the elastic theory.

From Figures 2a and 2c, deviatoric cyclic stress over deviatoric strain (i.e., σ_d/ε_d) has a nonlinear relation. Second, physical nonlinearity of σ_d/ε_d is a function of N and ε_d. The ratio of σ_d/ε_d decreases when both the repetition N and strain ε_d increase, which means the ratio σ_d/ε_d is softened with an increase of N and strain ε_d. If one similarly assumes the nonlinearity relation given by Li (1999a, 1999b) leads to the following expression for $\sigma_d / \varepsilon_d - N - \varepsilon_d$:

$$\sigma_d / \varepsilon_d = k_0 N^{k_2} \varepsilon_d^{k_3} . \tag{18}$$

The calibrated coefficients of k_0, k_2, and k_3 are calibrated and listed in Tables 3a and 3b. The same tow steps used to calibrate the parameters b_i (i = 0, 2, 3) are applied herein. Equation 18 clearly states that the ratio σ_d/ε_d changes with loading repetition N and deviatoric strain ε_d. When constitutive parameters k_2 and k_3 are both less than zero, σ_d/ε_d decreases with N and ε_d; otherwise, σ_d/ε_d increases. Since the value of k_3 does not change very much (see Table 3a), if the average value of k_3 is taken from each group, the ratio σ_d/ε_d versus ε_d for the two groups is given as follows:

Group DJ0: $$\sigma_d / \varepsilon_d = 59092 N^{-0.38} \varepsilon_d^{-0.23} \quad \text{(kPa)} \tag{19a}$$

Group DJ50: $$\sigma_d / \varepsilon_d = 9087 N^{-0.34} \varepsilon_d^{-0.49} \quad \text{(kPa).} \tag{19b}$$

The above expressions show the characteristics of physical nonlinearity associated with the power function that is changing with variables N and ε_d. Compared with the nonlinear elastic case investigated by Li (1999a), Equations 19a and 19b state that the resilient modulus declines with an increase of loading time and large deformation due to the structural damages of the subgrade material.

Shear Stress as a Function of N and ε_d

Figures 3a through 3d demonstrate the relation of stress-strain. Changes in stress similarly follow the pattern of the power function. From these results, it is evident that parameter n_3 controls the nonlinearity of stress-strain relation as soil skeletal deforms, whereas the parameter

n_2 dominates the nonlinear effect due to the cyclic shearing effect. The following two expressions are based on test data and calibrated parameters listed in Tables 4a and 4b:

Group DJ0: $$\sigma_d = 59092 N^{-0.38} \varepsilon_d^{0.75} \quad \text{(kPa)} \tag{20a}$$

Group DJ50: $$\sigma_d = 9087 N^{-0.34} \varepsilon_d^{0.51} \quad \text{(kPa).} \tag{20b}$$

Comparing Equation 19 to Equation 20, it is evident that calibrated parameters n_2 and n_3 match the calculated values ($n_2 = k_2 + 1 = 0.77$ and $n_3 = k_3 + 1 = 0.51$) well for the two groups. The larger absolute values of n_2 (or b_2) show higher structural sensitivity under cyclic loading.

Correlation of Stress Over Strain (σ / ε_d) and Stress Over Strain Rate ($\sigma / \dot{\varepsilon}_d$)

As described previously, the general nonlinear viscous model is shown in Equation 12, in which the equivalent effect of elasto-viscous behavior has also been illustrated. In Equation 13, the correlation between **D** and **D** dot (**D** dot is the time derivative of **D**) can be mathematically derived by taking the time derivative from the suggested constitutive law. For instance, taking the time derivative of shear viscosity leads to the following relation

$$\dot{\mu} = \dot{\mu}(N)\dot{N}\mu(I_1)\mu(J_2^D). \tag{21a}$$

Recalling the simplified form of Equation 8b with the assumptions of no effect of stress invariance I_1 in a quasi-triaxial space allows Equation 21a to be written as:

$$\dot{\mu} = (b_0 T / N) N^{b_2} \varepsilon_d^{b_3} = T / N\mu, \tag{21b}$$

where $N = t/T$, and T is the period of cyclic loading. At the same time, Equation 21 can be associated with Equation 8 by a function $C(N, \varepsilon_d)$ by the following relation:

$$(b_0 T / N) N^{b_2} \varepsilon_d^{b_3} = C(N, \varepsilon_d) k_0 N^{k_2} \varepsilon_d^{k_3} \tag{22}$$

or

$$C(N, \varepsilon_d) = (b_0 T / k_0 N) N^{b_2 - k_2} \varepsilon_d^{b_3 - k_3} \tag{23}$$

From Tables 2 through 4, differences of parameters (i.e., $b_2 - k_2$ and $b_3 - k_3$) are significantly small. Equation 23, therefore, can be further simplified to:

$$C(N,\varepsilon_d) = (b_0 T / k_0 N) . \quad (24)$$

From Equation 22, if the function $C(N, \varepsilon_d)$ in Equation 24 is a constant (i.e., b_0T/k_0N = constant), then shear viscosity is proportional to elastic shear modulus. Equation 24 suggests that, if the function $C(N, \varepsilon_d)$ becomes a constant, the parameters b_0 and k_0 are required to be a function of N to keep the ratio (i.e., b_0T/k_0N) in Equation 24 as a constant. This is an interesting topic and is recommended for future research.

Two groups of samples (DJ0 and DJ50) were tested, respectively, under two different confining pressures (i.e., confining pressure = 0.0 and 50 kPa). Note the difference in the relation of stress-N-strain relation from Figures 1 to 3. The effect of confining pressure at the low level is not significant.

Applications of the Results from the Experimental Investigations

The three relations presented in the previous discussion are: $\sigma_d / \dot{\varepsilon}_d - N - \varepsilon_d$, $\sigma_d / \varepsilon_d - N - \varepsilon_d$, and $\sigma_d - N - \varepsilon_d$, which are shown as a power function of N and strain ε_d. It is significant in the roadbed design to consider factors of nonlinearity related to the loading repetition and deviatoric strain. Before applying the above relations to the design of roadbed, investigate the loading characteristics related to the pattern of traffic flow. For example, study the response spectrum of dynamic loading induced within roadbed by vehicles. The traffic-induced loading may be associated with a certain pattern of traffic flow. Second, by applying a similar method adopted in earthquake engineering (e.g., the equivalent energy method) to the vehicle-induced load-time history curve, the random loading curve can be converted into a uniform and periodic loading sequence like that used in the laboratory. The detailed procedure of the conversion will not be

discussed in herein because it is out of the scope of this paper. Once the equivalent loading sequence has been identified, the viscosity can be found using Equation 17, combined with deformation at the point of failure. One can find the resilient modulus invoking Equation 19 if the nonlinear elastic theory is introduced.

SUMMARY AND CONCLUSIONS

Based on results discussed in this paper, the following conclusions are drawn:

1. A new nonlinear viscous model has been introduced in this paper. This is the first attempt to introduce a nonlinear viscous model for the investigations of subgrade soils under cyclic loading. The relationship between shear stress and shear strain rate is emphasized. In this model, the nonlinearity of shear viscosity is associated with deviatoric strain and repetition of cyclic loading. Since the introduced model can be considered as a time-dependent model, it is a powerful tool to predict the performance of subgrade soil with consideration of dynamic effect related to time, such as fatigue and creeping. A simplified case in a quasi-triaxial space has been discussed for convenience of further experimental investigations.

2. In this model, shear viscosity is our main concern. There are three constitutive parameters for shear viscosity (b_0, b_2, and b_3) that are calibrated in a pattern of the power function with test results from triaxial shear tests in Figures 1a through 1d. The parameters b_1 and b_3, respectively, carry information of the viscous nonlinearity related to soil deformation and structural damage. When constitutive parameters b_2 and b_3 are negligibly small, the nonlinear viscous model reduces to a linear model. Test results are based on two groups of subgrade samples collected from different sites.

3. Three sets of nonlinear relations are characterized from two groups of samples, namely stress over strain rate versus strain rate ($\sigma_d / \dot{\varepsilon}_d - N - \varepsilon_d$), stress over strain versus strain ($\sigma_d / \varepsilon_d - N - \varepsilon_d$), and stress versus strain ($\sigma_d - N - \varepsilon_d$). The related parameters (e.g., b_i, k_i and n_i, where i = 0, 2, and 3) are calibrated and listed in Tables 2 through 4. Test data and trend curves are plotted in Figures 1 through 3. A new expression of shear viscosity is essential in this research. The shear viscosity μ is introduced as a function of recoverable strain and the number of repetitions. Such an expression [i.e., $\mu = \mu(N, \varepsilon_d)$] provides a powerful tool for analysis of viscous behavior and dynamic response in pavement design, especially when information concerning deformation and repetitions is known. Furthermore, due to the feature of the relation as a function of stress, strain, strain rate, and time, there are opportunities for further

research in rheological characteristics, such as failure due to fatigue and creeping within subgrade layers.

4. Correlation between nonlinear shear viscosity and elastic modulus is discussed. Shear viscosity and shear modulus are both functions of deviatoric strain and repletion N and change with N and ε_d with the same pattern. Both decrease with N and ε_d with a power function. For the relation of stress versus strain, stress also decreases with an increase of the repetition N, but stress increases with increase of strain in a power function. A function $C(N, \varepsilon_d)$ is introduced to link the nonlinear viscosity and modulus. In this investigation, it is found that, when $C(N, \varepsilon_d)$ becomes a constant, shear viscosity is proportional to the elastic modulus.
5. It should be pointed out that the research results from this investigation not only can be applied to designs of pavement roadbed, but also can be used in other highway system projects. For example, the nonlinear behavior of soil plays a role in bridge foundations or slopes in highway systems.

In brief, enhancing our understanding of viscous behavior and dynamic response of subgrade soils is essential and important in highway design. The findings from this research will apply to and improve the design in a highway system; and in the long run, it will also benefit the performance of infrastructures in terms of longer life and lower cost of maintenance.

NOMENCLATURE

a_i	bulk viscous constitutive parameters (i = 0, 1, 2, and 3)
b_i	shear viscous constitutive parameters (i = 0, 1, 2, and 3)
$\mathbf{b}$	body force vector, kg/m^2 - sec^2
c_i	parameters in the governing equation (i = 1, 2, 3, 4, and 5)
$\mathbf{D}$	a fourth-order tensor of viscosity, kg/m-sec
$\mathbf{I}_1$	the first invariance of stress, kg/m-sec^2
$\mathbf{J}_2^D$	the second deviatoric invariance of train
k_i	constitutive parameters (i = 0, 1, 2, and 3)
$\mathbf{L}$	a matrix to convert displacement into strain tensor, 1/m
n	porosity
n_i	constitutive parameters (i = 0, 1, 2, and 3)
M_r	resilient modulus, kg/m-sec^2
N	the number of repetitions
$\mathbf{q}^b$	the bulk flux, m/sec
$\mathbf{R}$	the vector in the governing equation, kg/m^2-sec^2
t	time, sec
$\mathbf{u}$	displacement, m
$\mathbf{v}_S$, $\mathbf{v}_W$	average phase velocities of the solid matrix and water, m/sec
$\mathbf{v}_r$	relative velocity between the solid and fluid phases ($\mathbf{v}_W - \mathbf{v}_S$), m/sec
$\boldsymbol{\delta}$	the Kronecker delta
$\boldsymbol{\varepsilon}_I$	the principal strain (i = 1, 2, and 3)
ε_d	deviatoric strain
$\boldsymbol{\varepsilon}$	structural infinitesimal strain tensor
$\boldsymbol{\varepsilon}^D$	deviatoric infinitesimal strain tensor
$tr\boldsymbol{\varepsilon}$	trace of structural infinitesimal strain tensor

γ_w	unit weight of water, kg/m^2-sec^2
κ, μ	nonlinear bulk and shear viscosity parameters, kg/m-sec
ρ_S	phase densities of individual solid grains, kg/m^3
$\boldsymbol{\sigma}_d$	deviatoric stress, kg/m-sec^2
$\boldsymbol{\sigma}_i$	the principal stress (I = 1, 2, and 3), kg/m-sec^2
$\boldsymbol{\sigma}$	the structural stress tensor, kg/m-sec^2
$\boldsymbol{\sigma}^D$	the deviatoric stress tensor, kg/m-sec^2
$tr\boldsymbol{\sigma}$	the trace of stress structural tensor, kg/m-sec^2

d/dt	total derivative with respect to time t, 1/sec
∇	derivative operator for gradient, divergence, and curl, 1/m
$\partial/\partial t$	partial derivative with respect to time, 1/sec
$\dot{\ }$	dot for time derivative

<u>superscripts</u>

D	deviatoric
r	relative
s	solid
w	water
$\dot{\ }$	dot for time derivative

<u>subscripts</u>

d	deviatoric
s	solid
w	water
0	initial state at time t = 0

REFERENCES

AASHTO. *Guide for Design of Pavement Structures*, Vols. 1 and 2, AASHTO, Washington, DC, 1986/1993.

Heydinger, A. G., Q. Xie, B. W. Randolph, and J. D. Gupta. Analysis of Resilient Modulus of Dense- and Open-Grade Aggregates, *Transportation Research Record*, 1547, TRB, National Research Council, Washington, DC, 1996, pp. 1–12.

Li, J. Investigation for Constitutive Behavior of Granite Residual Soil under Cyclic Loading, in S. Wang (ed.): *Advances in Geological Engineering*, Proceedings of the International Symposium on Advances in Geological Engineering, Beijing, China, 1990, pp. 111–116.

Li., J. Constitutive Law for Saturated Soil with Non-Newtonian Behavior, in W. Zhu (ed.): *Geomechanics and Engineering Application*, Proceedings of the Chinese Young Scholar Symposium on Geomechanics and Engineering Application, Chinese Academy of Science, Wuhan, China, Science Press, 1994, pp. 770–775.

Li, J. Experimental Investigations of Nonlinear Elastic Behavior of Subgrade Soils under Traffic-induced Loading, Research Report of the National Transportation Center, Morgan State University, Baltimore, MD, 1999a, pp. 32.

Li, J. Nonlinear Elastic Behavior of Subgrade Soils under Traffic Loading, in Proceedings of the XII European Conference on Soil Mechanics and Geotechnical Engineering, Geotechnical Engineering for Transportation Infrastructure, Amsterdam, the Netherlands, 1999b, CD-ROM, Author No. 305, Session No. 3.2.

Li, J. Experimental Investigations of Nonlinear Viscous Soils, in Proceedings of the Fourth International Conference on Constitutive Laws for Engineering Materials: Experiment, Theory, Computation and Applications, Troy, NY, 1999c, pp. 359–362.

Li, J., and D.C. Helm. A General Formulation for Aquifer Deformation under Dynamic and Viscous Conditions, in F. B. J. Barends, F. J. J. Brouwer, and F. H. Schroder (eds.): *Land Subsidence*, International Association of Scientific Hydrology, Proceedings of the Fifth International Symposium on Land Subsidence, The Hague, the Netherlands, 1995, pp. 323–332.

Li, J., and D.C. Helm. A Theory for Dynamic Motion of Saturated Soil Characterized by Viscous Behavior, in J. Borchers (ed.): *Land Subsidence Case Histories and Current Research: Proceedings of the Dr. Joseph F. Poland Symposium on Land Subsidence*, Association of Engineering Geologists Special Publication No. 8, 1998, pp. 356–407.

Malvern, L. E. *Introduction to the Mechanics of a Continuous Medium*, Prentice-Hall, Englewood Cliffs, NJ, 1969.

Mohamad, L. N., J. Puppala, and P. Alavilli. Resilient Properties of Laboratory Compacted Subgrade Soils, *Transportation Research Record*, 1504, TRB, National Research Council, Washington, DC, 1995, pp. 87–102.

Nazarian, S., R. Pezo, S. Melarkode, and M. Picornell. Testing Methodology for Resilient Modulus of Base Materials, *Transportation Research Record*, 1547, TRB, National Research Council, Washington, DC, 1996, pp. 47–85.

Nunes, M. C. M., and A. R. Dawson. Behavior of Sonme Pavement Foundation Material under Repeated Loading, *Transportation Research Record*, 1577, TRB, National Research Council, Washington, DC, 1997, pp. 1–9.

Ping, W. V., and L. Ge. Field Verification of Laboratory Resilient Modulus Measurement on Subgrade Soils, *Transportation Research Record*, 1577, TRB, National Research Council, Washington, DC, 1997, pp. 53–61.

Ping, W. V. and L. Ge. Evaluation of Resilient Modulus of Cement Lime Rock Base Material in Florida, *Transportation Research Record*, 1546, TRB, National Research Council, Washington, DC, 1996, pp. 1–12.

Zienkiewicz, O. C. *The Finite Element Method* (3rd edition), McGraw-Hill, NY, 1977.

Table 1a Physical Properties of Subgrade Samples

Sample Name	Optimum Water Content (%)	$\gamma_{soil\ wet}$ (10^{-3} kN/m^3)	Plastic Limit (%)	Liquid Limit (%)	Classification (AASHTO)
DJ-1	14.0	16.66	5.0	30.0	A4
DJ-2	14.0	16.66	5.0	30.0	A4
DJ-3	14.0	16.66	5.0	30.0	A4
DJ-4	14.0	16.66	5.0	30.0	A4
DJ-5	14.0	16.66	5.0	30.0	A4
DJ-6	14.0	16.66	5.0	30.0	A4

Table 1b Test Conditions

Sample No.	Cycles No. in Sequence	Load Time (s)	Cycle Time (s)	Sitting Load (kPa)	Confining Pressure (kPa)	Loading Wave Type
DJ-1	50	0.25	1.0	10.0	0.0	Havesine
DJ-2	200	0.25	1.0	10.0	0.0	Havesine
DJ-3	500	0.25	1.0	10.0	0.0	Havesine
DJ-4	10	0.25	1.0	10.0	50.0	Havesine
DJ-5	50	0.25	1.0	10.0	50.0	Havesine
DJ-6	500	0.25	1.0	10.0	50.0	Havesine

Table 2a Calibration of Parameters b_0, b_2, and b_3

Sample No.	$b_0 f(N)$ (kPa)	b_3	N_i	R^2
DJ-1	3321	-0.20	50	0.944
DJ-2	1460	-0.24	200	0.967
DJ-3	1277	-0.26	500	0.997
DJ-4	898	-0.46	10	0.97
DJ-5	692	-0.48	50	0.99
DJ-6	247	-0.55	500	0.99

Table 2b Calibration of Parameters b_0, b_2, and b_3

Sample No.	$f(N)$	b_0 (kPa)	b_2	R^2	Confining Pressure (kPa)
DJ0	$b_0 N^{b_2}$	16706	–0.43	0.999	0.0
DJ50	$b_0 N^{b_2}$	2172	–0.34	0.950	50.0

Table 3a Calibration of Parameters k_0, k_2, and k_3

Sample No.	$k_0 N^{k2}$ (kPa)	k_3	N_i	R^2
DJ-1	13282	–0.20	50	0.94
DJ-2	7616	–0.24	200	0.97
DJ-3	5514	–0.26	500	0.99
DJ-4	3595	–0.46	10	0.97
DJ-5	3051	–0.47	50	0.99
DJ-6	989	–0.55	500	0.99

Table 3b Calibration of Parameters k_0, k_2, and k_3

Sample No.	$f(N)$	k_0 (kPa)	k_2	R^2	Confining Pressure (kPa)
DJ0	$k_0 N^{k_2}$	59092	–0.38	0.99	0.0
DJ50	$k_0 N^{k_2}$	9087	–0.34	0.91	50.0

Table 4a Calibration of Parameters n_0, n_1, and n_3

Sample No.	$n_0 f(N)$ (kPa)	n_3	N_i	R^2
DJ-1	14517	0.86	50	0.997
DJ-2	7616	0.76	200	0.997
DJ-3	2424	0.62	500	0.990
DJ-4	2201	0.47	10	0.93
DJ-5	5069	0.60	50	0.97
DJ-6	990	0.46	500	0.99

Table 4b Calibration of Parameters n_0, n_2, and n_3

Sample No.	$f(N)$	n_0(kPa)	n_2	R^2	Confining Pressure (kPa)
DJ0	$n_0N^{n_2}$	17327	–0.004	0.99	0.0
DJ50	$n_0N^{n_2}$	5994	–0.24	0.33	50.0

Figure 1a **Stress over strain rate versus strain $(\sigma_d / \dot{\varepsilon}_d - \varepsilon_d)$ for Group DJ0**

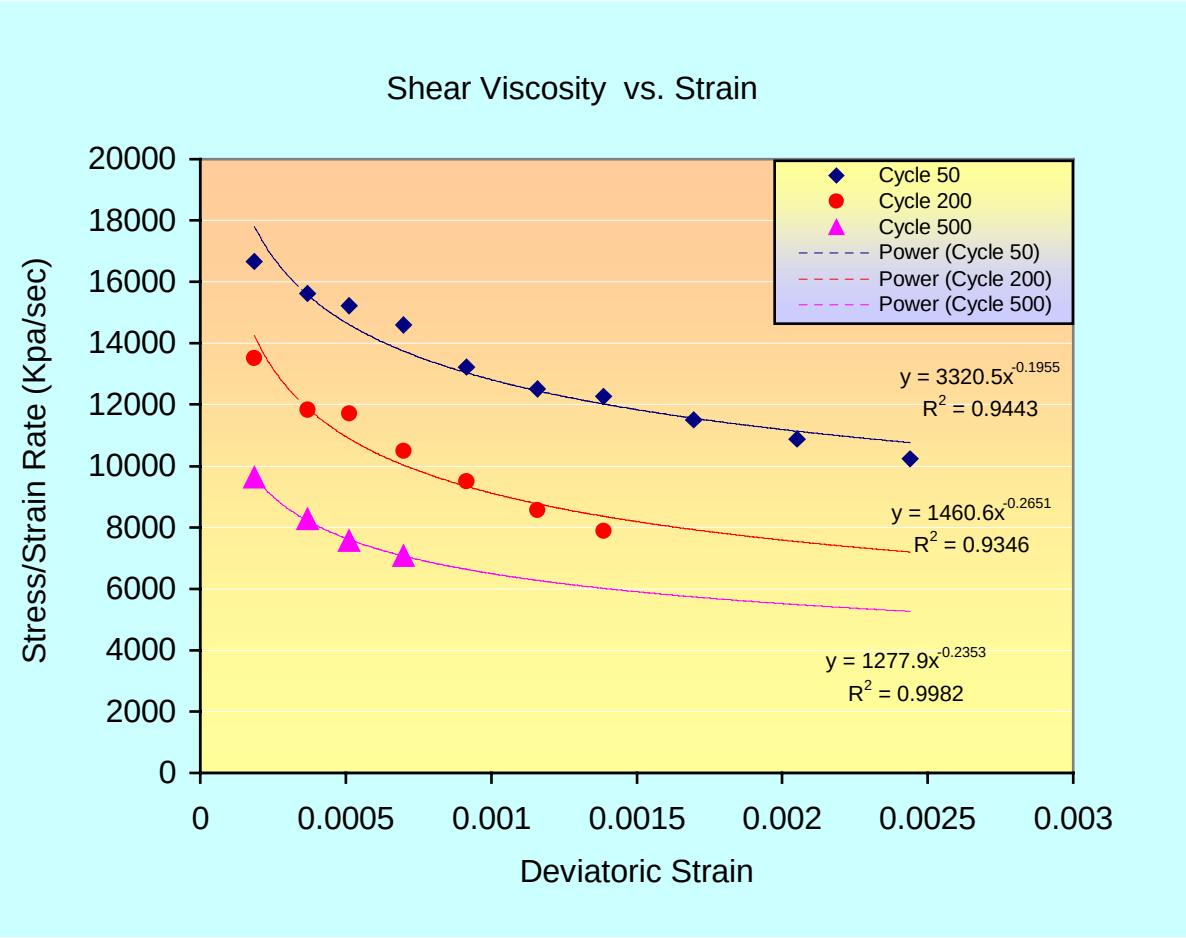

Figure 1b Calibration of parameters (b_0 and b_2) for Group DJ0

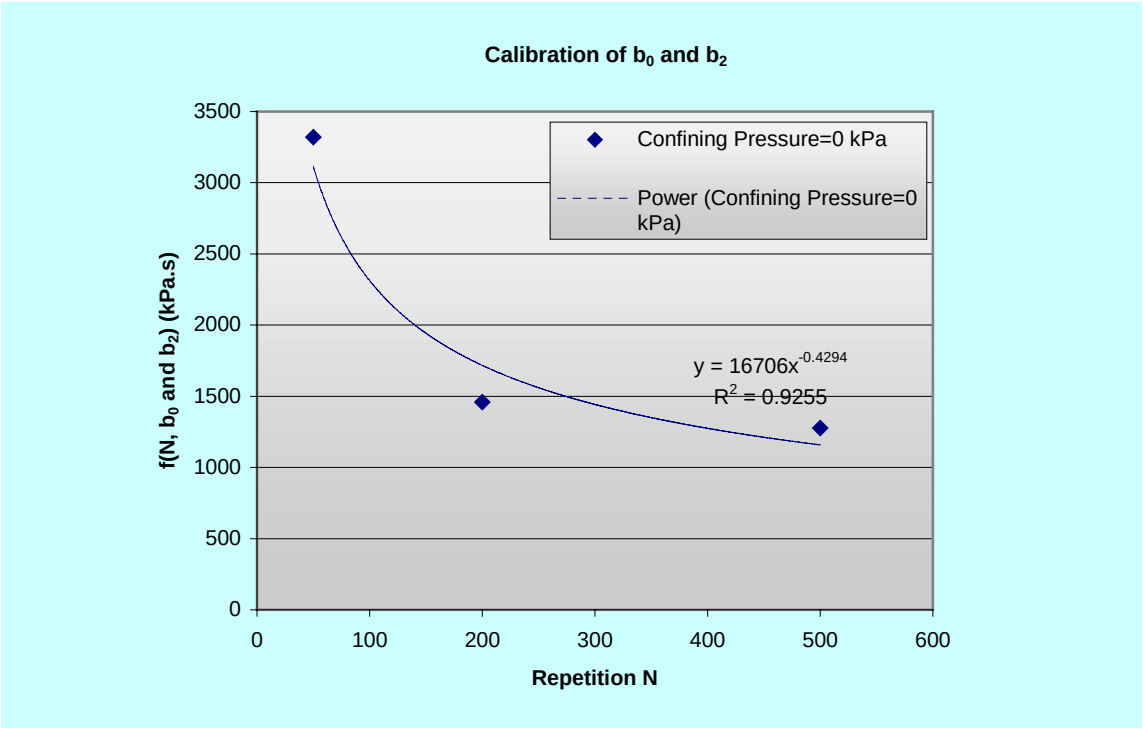

Figure 1c Stress over strain rate versus strain $(\sigma_d / \dot{\varepsilon}_d - \varepsilon_d)$ for Group DJ50

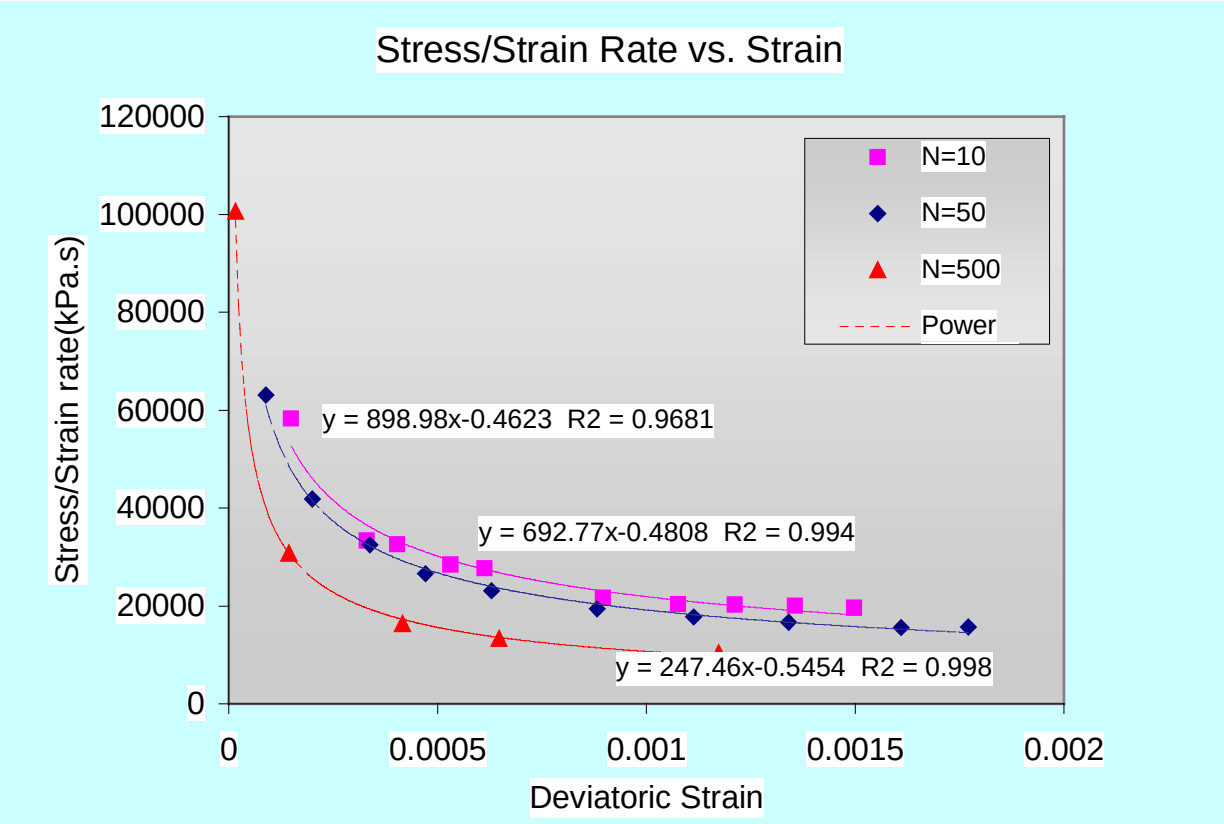

Figure 1d Calibration of parameters (b_0 and b_2) for Group DJ50

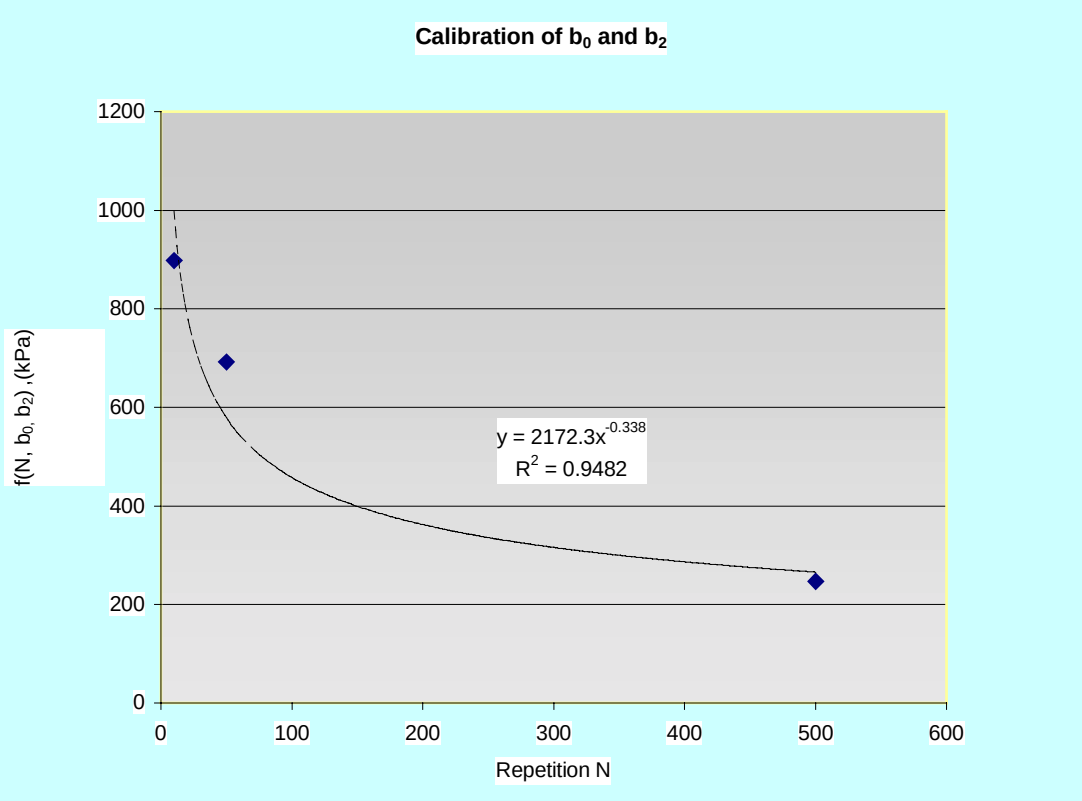

Figure 2a **Stress over strain versus strain $(\sigma_d / \varepsilon_d - \varepsilon_d)$ for Group DJ0**

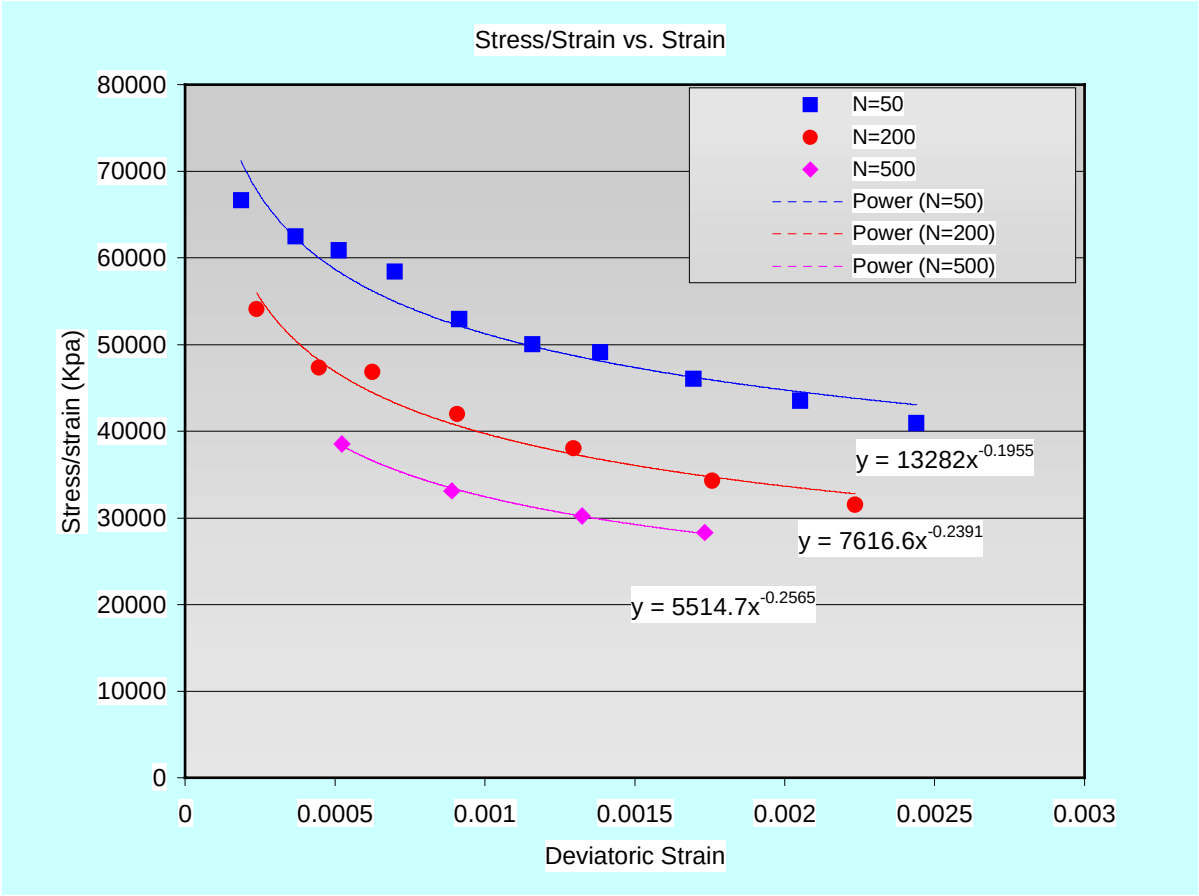

Figure 2b Calibration of parameters (k_0 and k_2) for Group DJ0

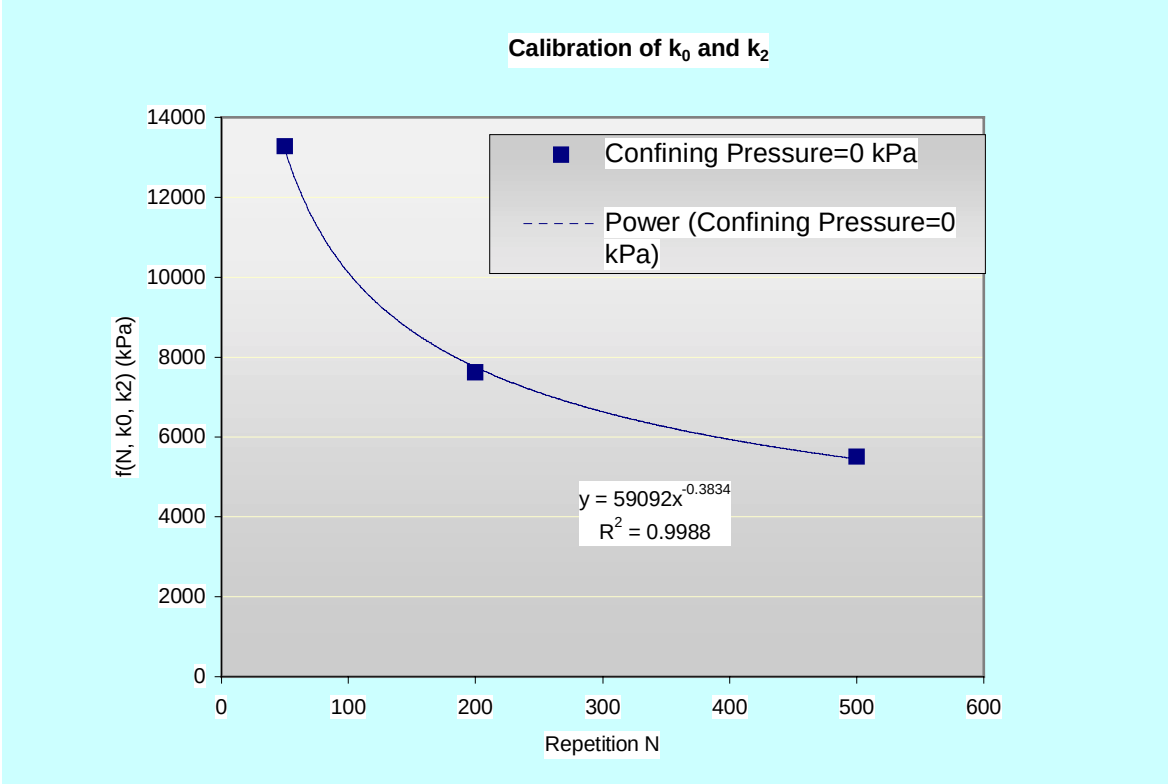
Calibration of k_0 and k_2
14000
12000
10000
8000
6000
4000
2000
0
f(N, k0, k2) (kPa)
0
100
200
300
400
500
600
Repetition N
Confining Pressure=0 kPa
Power (Confining Pressure=0 kPa)
$y = 59092x^{-0.3834}$
$R^2 = 0.9988$

Figure 2c Stress over strain versus strain $(\sigma_d / \varepsilon_d - \varepsilon_d)$ for Group DJ50

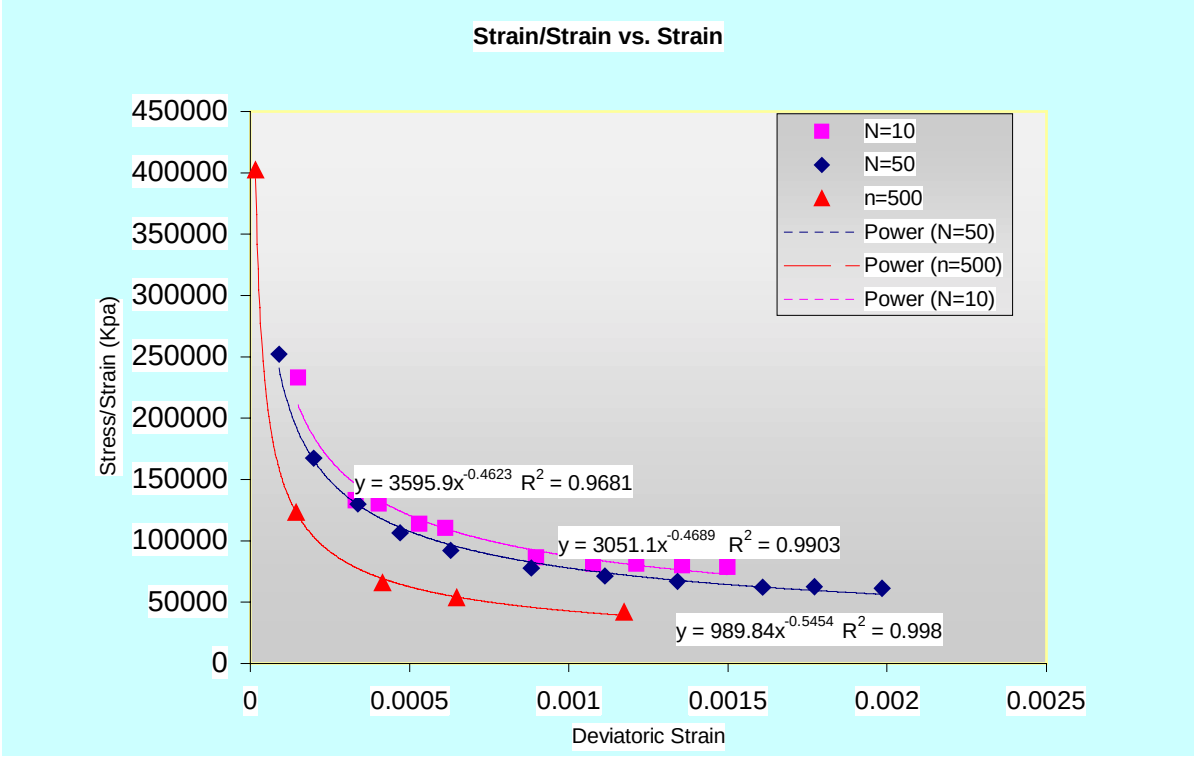

Figure 2d Calibration of parameters (k_0 and k_2) for Group DJ50

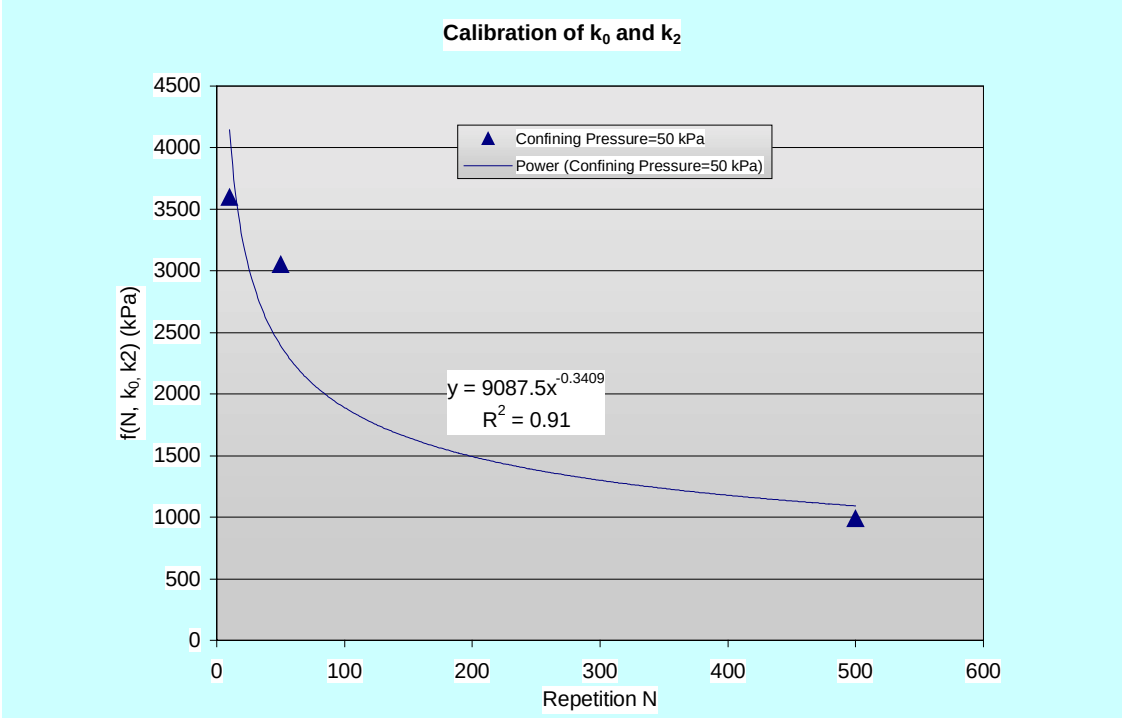

Figure 3a Stress versus strain $(\sigma_d - \varepsilon_d)$ for Group DJ0

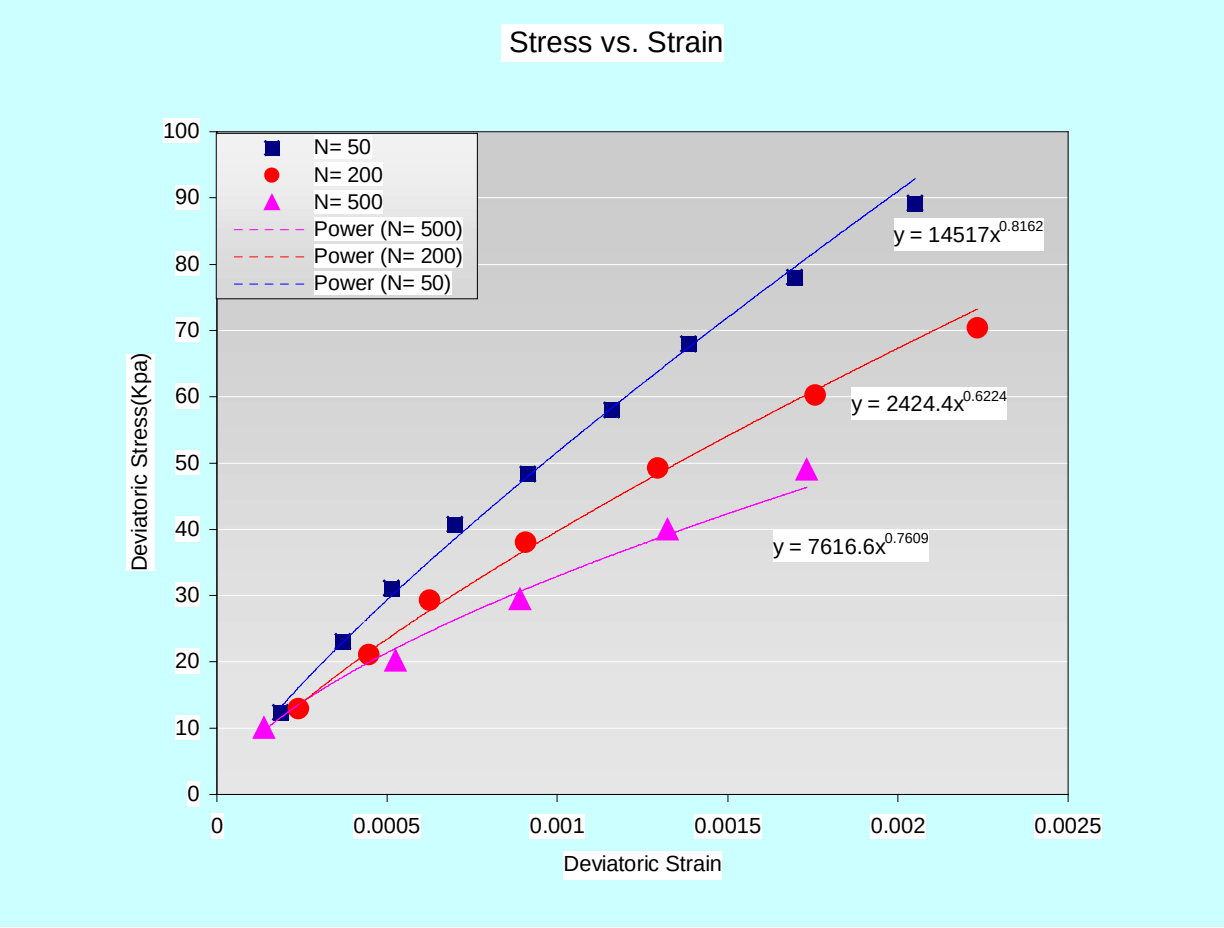

Figure 3b Calibration of parameters (n_0 and n_2) for Group DJ0

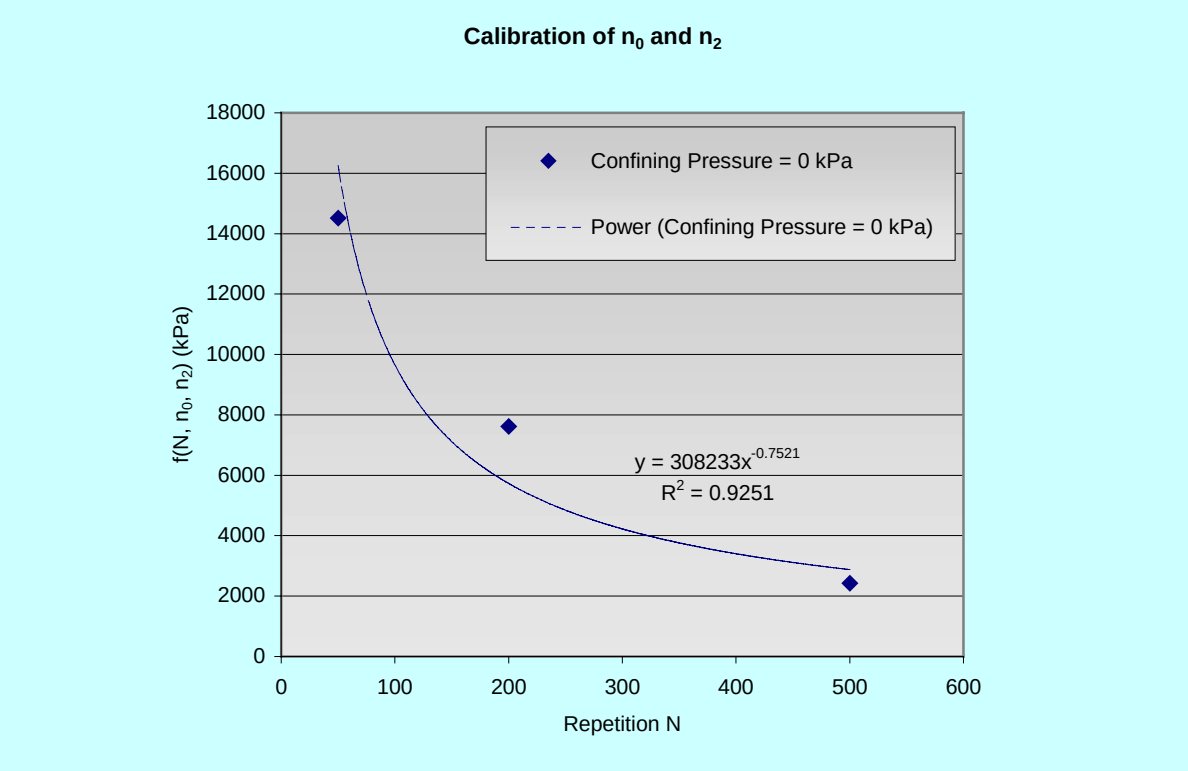

Figure 3c Stress versus strain $(\sigma_d - \varepsilon_d)$ for Group DJ50

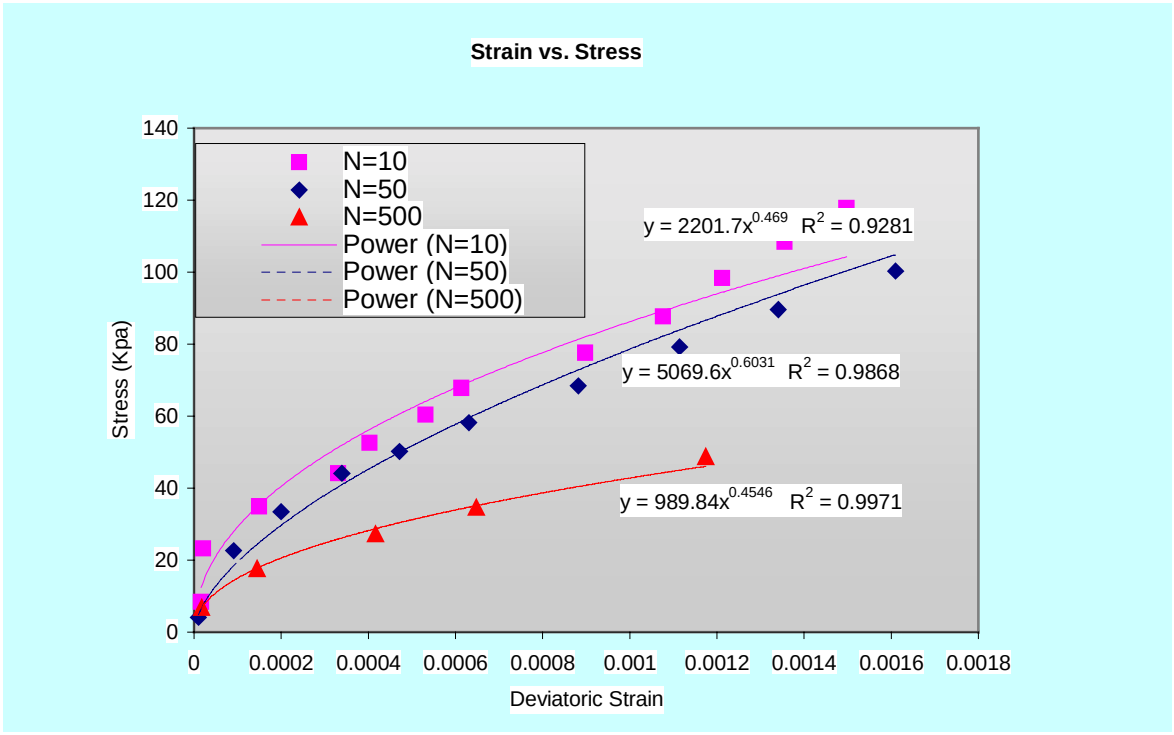

Figure 3d Calibration of parameters (n_0 and n_2) for Group DJ50